Human Molecular Genetics, 2011, Vol. 20, No. 9 ***1820–1833***
doi:10.1093/hmg/ddr065
Advance Access published on February 14, 2011

Puromycin-sensitive aminopeptidase (PSA/NPEPPS) impedes development of neuropathology in hPSA/TAU^{P301L} double-transgenic mice

Lili C. Kudo[1,†], Liubov Parfenova[2,†], Guijie Ren[2,3], Nancy Vi[1], Maria Hui[4], Zhongcai Ma[2], Kimbley Lau[2], Michelle Gray[5], Fawzia Bardag-Gorce[6], Martina Wiedau-Pazos[7], Koon-Sea Hui[4] and Stanislav L. Karsten[1,2,7,*]

[1]NeuroInDx Inc., 1655 East 28th Street, Signal Hill, CA 90755, USA, [2]Division of Neuroscience, Department of Neurology, Los Angeles Biomedical Research Institute at Harbor-UCLA Medical Center, Torrance, CA 90502, USA, [3]Department of Biochemistry and Molecular Biology, Medical College, Shandong University, Jinan 250012, P.R. China, [4]Nathan S. Kline Institute for Psychiatric Research, New York University School of Medicine, Orangeburg, NY 10962, USA, [5]Department of Neurology, UAB School of Medicine, University of Alabama at Birmingham, Birmingham, AL 35294-0021, USA, [6]Department of Pathology and Laboratory Medicine, Harbor-UCLA Medical Center, 1124 West Carson Street, Torrance, CA 90502, USA and [7]Department of Neurology, David Geffen School of Medicine at UCLA, Los Angeles, CA 90095, USA

Received November 19, 2010; Revised and Accepted February 10, 2011

Accumulation of neurotoxic hyperphosphorylated TAU protein is a major pathological hallmark of Alzheimer disease and other neurodegenerative dementias collectively called tauopathies. Puromycin-sensitive aminopeptidase (PSA/NPEPPS) is a novel modifier of TAU-induced neurodegeneration with neuroprotective effects via direct proteolysis of TAU protein. Here, to examine the effects of PSA/NPEPPS overexpression *in vivo* in the mammalian system, we generated and crossed BAC-PSA/NPEPPS transgenic mice with the TAU^{P301L} mouse model of neurodegeneration. PSA/NPEPPS activity in the brain and peripheral tissues of human PSA/NPEPPS (hPSA) mice was elevated by ~2–3-fold with no noticeable deleterious physiological effects. Double-transgenic animals for hPSA and TAU^{P301L} transgenes demonstrated a distinct trend for delayed paralysis and showed significantly improved motor neuron counts, no gliosis and markedly reduced levels of total and hyperphosphorylated TAU in the spinal cord, brain stem, cortex, hippocampus and cerebellum of adult and aged animals when compared with TAU^{P301L} mice. Furthermore, endogenous TAU protein abundance in human neuroblastoma SH-SY5Y cells was significantly reduced or augmented by overexpression or knockdown of PSA/NPEPPS, respectively. This study demonstrated that without showing neurotoxic effects, elevation of PSA/NPEPPS activity *in vivo* effectively blocks accumulation of soluble hyperphosphorylated TAU protein and slows down the disease progression in the mammalian system. Our data suggest that increasing PSA/NPEPPS activity may be a feasible therapeutic approach to eliminate accumulation of unwanted toxic substrates such as TAU.

INTRODUCTION

Tauopathies are a group of neurodegenerative disorders, including Alzheimer's disease (AD), which are characterized by abnormal accumulation of hyperphosphorylated TAU protein in the form of neurofibrillary tangles (NFTs) (1). Reduction of pathologically accumulating toxic TAU may offer a compelling potential therapy for AD and other

*To whom correspondence should be addressed at: 1124 West Carson Street, Torrance, CA 90509, USA. Tel: +1 3107811477; Email: skarsten@ucla.edu
†These authors contributed equally and are listed in alphabetical order.

tauopathies (2,3). However, little is known about the pathways involved in TAU protein clearance. Recently, we have identified a novel pathway of TAU protein processing involving puromycin-sensitive aminopeptidase (PSA/NPEPPS), and demonstrated the ability of PSA/NPEPPS to protect from TAU-induced neurodegeneration *in vivo* in the *Drosophila* model (4,5). The role of human PSA/NPEPPS (hPSA) as a TAU aminopeptidase was confirmed in a cell-free system (4). Yet, the question of whether PSA/NPEPPS has similar neuroprotective properties in mammals remained unanswered.

PSA/NPEPPS (EC 3.4.11.14), originally described as MP100 (6), is a conservative aminopeptidase that hydrolyzes N-terminal amino acids and belongs to the M1 metalloprotease family (7,8). PSA/NPEPPS is mainly a cytoplasmic protein that is most abundant in the brain (9,10). One of the first putative PSA/NPEPPS functions was its potential role in the degradation of enkephalins, and as such was considered an enkephalinase (6). However, its intracellular localization (7,9,11) and the lack of detectable changes in enkephalin expression in PSA/NPEPPS-deficient ($PSA^{goku/goku}$) mice (12) suggest a different function for PSA/NPEPPS.

Indeed, PSA/NPEPPS may have other functions in the central nervous system (CNS). For example, it was demonstrated that PSA/NPEPPS is a major peptidase responsible for the degradation of polyglutamine repeats, implicating this enzyme in the pathogenesis of polyQ diseases, including Huntington disease (13). Another recent report links PSA/NPEPPS function to autophagy and demonstrates its ability to facilitate removal of other neurotoxic substrates such as polyQ-expanded huntingtin exon-1, ataxin-3, mutant α-synuclein and SOD1 (14).

In addition to its putative neuroprotective role in both flies and mammals (4,13,14), PSA/NPEPPS was implicated in cell cycle regulation in mammals (7), meiotic exit in *C. elegans* (15,16) and MHC class I peptide presentation (17). PSA/NPEPPS knockout mice are smaller and have deficient reproductive function (17), confirming its role previously reported in spermatogenesis (15). Both PSA/NPEPPS-deficient mice, $PSA^{goku/goku}$ (12), and knockout mice (17) have neurological abnormalities notable in deficient locomotor activity (movement disorder of hind limbs) and increased anxiety, which once again points to the importance of the role of PSA/NPEPPSs in the CNS.

Here, to examine the effects of PSA/NPEPPS on the progress of TAU-induced neurodegeneration *in vivo* in mammals, we generated two independent lines of bacterial artificial chromosome (BAC) transgenic mice overexpressing hPSA and crossed them with a well-established model of TAU-induced neurodegeneration, TAU^{P301L} transgenic mice (18). PSA/NPEPPS transgenic mice were generated using BAC-mediated technology (19,20). Both lines of BAC-PSA/NPEPPS transgenic mice overexpressing hPSA are born normal, breed normally and do not reveal any gross anatomical or behavioral abnormalities. Expression and activity of hPSA were elevated in the brain and peripheral tissues of hemizygous hPSA mice from 2- to 3-fold compared with non-transgenic littermate controls. Double-transgenic animals for hPSA and TAU^{P301L} transgenes were characterized at 6, 9 and 15 months of age. hPSA/TAU^{P301L} mice showed delayed onset of disease phenotype, improved motor neuron counts and marked reduction of both total and hyperphosphorylated TAU protein in all tissues at all ages tested. These data demonstrate that hPSA/NPEPPS is a neuroprotective factor that directly acts on TAU protein and ameliorates TAU-induced neurotoxicity in mammals *in vivo*. Hence, PSA/NPEPPS activation may be a feasible therapeutic approach to treat age-related tauopathies including AD.

RESULTS

BAC hPSA transgenic mice demonstrate elevated PSA/NPEPPS enzyme activity but no gross abnormalities

Three independent lines of hPSA transgenic mice were generated using BAC-mediated technology (19,20). PSA/NPEPPS enzyme activity measurements in all three hPSA lines demonstrated 2–3-fold elevation in all brain regions tested (Fig. 1A) while the activities of other brain aminopeptidases, neuron specific aminopeptidase 1 and 2 (NAP1 and NAP2), were not altered (Supplementary Material, Fig. S1A and B). In addition, PSA/NPEPPS enzyme activity was consistently elevated in the muscle, kidney and liver of hPSA mice (Supplementary Material, Fig. S1C). On the basis of genotyping, PSA/NPEPPS activity measurements and western blot analyses (Fig. 1), two hPSA founder lines (hPSA1 and hPSA2) were expanded on the FvB background for at least 10 generations. hPSA mice expressed the PSA/NPEPPS transgene in the brain at levels roughly equivalent to 2-fold elevation compared with non-transgenic controls based on RNA and protein expression measurements (Table 1 and Fig. 1).

The litter size from transgenic pairs was on average eight to nine pups, not significantly different from non-transgenic controls. No significant difference in the mortality of pups between birth and weaning was noticed between hPSA and non-transgenic mice. Unlike PSA/NPEPPS-deficient mice characterized by a smaller body size and reduced testes (17,21,22), hPSA transgenic mice did not display any differences in size, had normal-size testes and did not exhibit any other gross anatomical abnormalities.

Overexpression of PSA/NPEPPS does not alter enkephalin degradation rates *in vivo*

To test the hypothesis that PSA/NPEPPS may function as enkephalinase, both lines of adult hPSA mice were tested for altered enkephalin degradation rates using Met-enkephalin (MEK) degradation assay. No significant changes in the enkephalin turnover/degradation rates were detected when brain extracts from non-transgenic controls were compared with hPSA1 ($P = 0.23$) and hPSA2 ($P = 0.27$) mice (Fig. 1D), supporting the notion that PSA is not a primary enkephalinase (7,9,11,12).

Overexpression of PSA/NPEPPS does not affect the activities of major protein processing and clearance systems *in vivo*

Recent reports implicated PSA/NPEPPS in interaction with proteasome- (13) or autophagy (14)-mediated protein clearance. To test whether elevation of PSA/NPEPPS expression

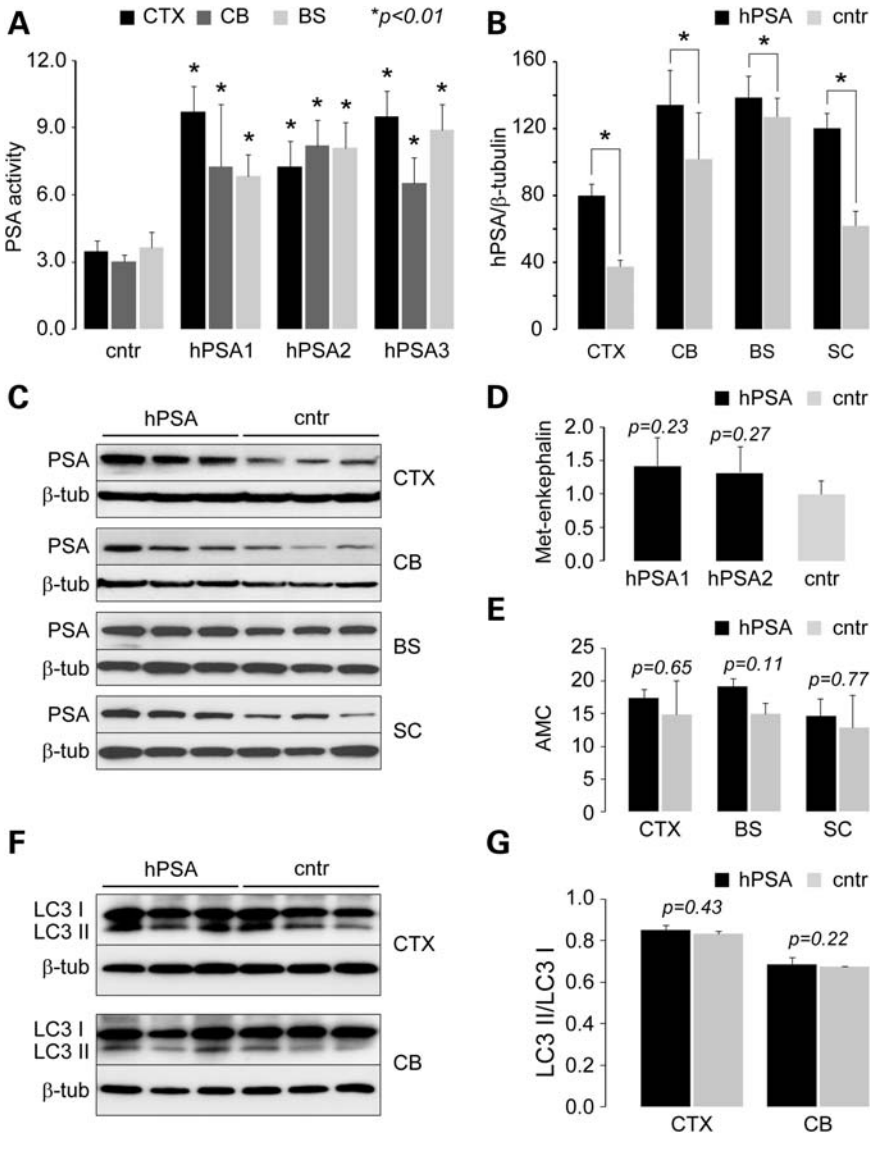

Figure 1. hPSA transgenic mouse lines demonstrate elevated PSA/NPEPPS enzyme activity and protein expression, while enkephalin degradation rates, proteosome and autophagy system activities are not significantly altered. (**A**) PSA activity measured in three independent hPSA transgenic lines (hPSA1, hPSA2 and hPSA3) demonstrates elevation of PSA activity from 2- to 3-fold in all brain regions and genetic lines. PSA/NPEPPS activity is shown in arbitrary units; (**B** and **C**) western blot analysis using anti-PSA/NPEPPS antibodies demonstrates elevation of PSA/NPEPPS protein expression in all brain regions of hPSA transgenic mice. (**D**) Enkephalin degradation rates are not significantly changed in the brain of 6-month-old hPSA1 and hPSA2 transgenic mice. (**E**) Proteasome activity measured with SucLeuLeuValTyr-AMC proteasome fluorogenic substrate is not significantly altered in all brain regions of 6-month-old hPSA mice analyzed. (**F** and **G**) Autophagy system activity measured by the relative ratio of LC3 II and LC3 I fragments is not altered in the adult hPSA mice. CTX, cortex; CB, cerebellum; BS, brain stem; SC, spinal cord; cntr, control non-transgenic littermates; β-tub, β-tubulin. Asterisks indicate $P < 0.01$.

affects the activities of these systems, several tests were carried out. The measurements of proteosome activity in the cortex, brain stem and cerebellum of adult hPSA mice (6 months) using SucLeuLeuValTyr-AMC proteasome fluorogenic substrate did not demonstrate any significant differences from the control non-transgenic littermate brain samples (Fig. 1E). Analysis of LC3-I (cytosolic) to LC3-II (autophagosome) relative ratios indicative of changes in autophagy system activity in the protein extracts isolated from the cortex and cerebellum of adult (6 months) hPSA and non-transgenic littermate mice also did not reveal any significant differences (Fig. 1F and G). Therefore, tests for both system activities measured in several brain regions of hPSA mice and compared with non-transgenic littermate controls (Fig. 1E–G) suggested that there is no direct functional link between hPSA/NPEPPS overexpression and ubiquitin-proteasome or autophagy system activities.

hPSA overexpression has moderate to no effect on brain transcriptome

Microarray-based transcriptome analysis of cortical and cerebellum transcriptomes identified 128 transcripts altered in at least one of the analyzed brain regions of

Table 1. Gene expression changes identified in the cortex (CTX) and cerebellum (CB) of adult (6-month-old) hPSA transgenic mice

GenBank	Gene	CTX	*P*-value	CB	*P*-value
NM_008942	PSA/NPEPPS, aminopeptidase puromycin sensitive	1.7	0.001	1.9	0.008
NM_007748	Cox6a1, cytochrome c oxidase, subunit VIa, polypeptide 1	2.2	0.0004	2.2	0.001
NM_018853	Rplp1, ribosomal protein, large, P1	1.9	0.001	1.6	0.0005
NM_008972	Ptma, prothymosin alpha	−1.8	0.003	−2.2	0.008
AF073993	Hnrpa2b1, heterogeneous nuclear ribonucleoprotein A2/B1	−1.5	0.0001	−1.7	0.009

CTX and CB columns represent average fold changes in the hPSA mice versus non-transgenic littermate controls. See the MIAME report for experimental details. Notice that PSA/NPEPPS is consistently elevated in both brain regions.

adult 6-month-old hPSA1 transgenic mice (see the MIAME report). These corresponded to 43 and 65 known genes regulated in the cortex and cerebellum, respectively. Five known genes/probes satisfied the selected criteria for regulation in both brain regions (Table 1). As expected, the PSA/NPEPPS transcript showed significant elevation in the cortex (1.72-fold; $P = 0.001$) and cerebellum (1.92-fold; $P = 0.008$) of hPSA mice. Higher expression of hPSA in the cerebellum compared with cortex was in agreement with previous mouse and human data (4). Gene Ontology (GO) analysis revealed that the biological processes most altered in the cortex or cerebellum of hPSA mice are those associated with the monosaccharide metabolic process (fold enrichment = 5.9, EASE = 0.001) and sex differentiation (fold enrichment = 6.1, EASE = 0.009).

Mouse endogenous TAU protein expression is not altered in hPSA transgenic mice

To evaluate whether endogenous murine TAU protein levels may be affected by the elevated expression of hPSA, we applied western blot and immunohistochemical analyses. T46 antibodies, which are specific for C-terminus of total TAU, were used for western blot analysis of protein extracts isolated from the cortex, brain stem, cerebellum and spinal cord of adult (6-month) hPSA and non-transgenic littermate controls. The results did not show any difference between hPSA and non-transgenic mouse tissues (Fig. 2A). Immunohistochemical analysis of spinal cord tissues using the same antibodies and same age mice also revealed no noticeable differences (Fig. 2B). To ensure that these results are not an artifact, additional V-20 antibodies were used, which also demonstrated no visible differences in staining between hPSA and control tissues (data not shown). These combined data demonstrate that hPSA transgenic mice have the same levels of TAU protein compared with non-transgenic littermate controls in all brain regions tested (Fig. 2).

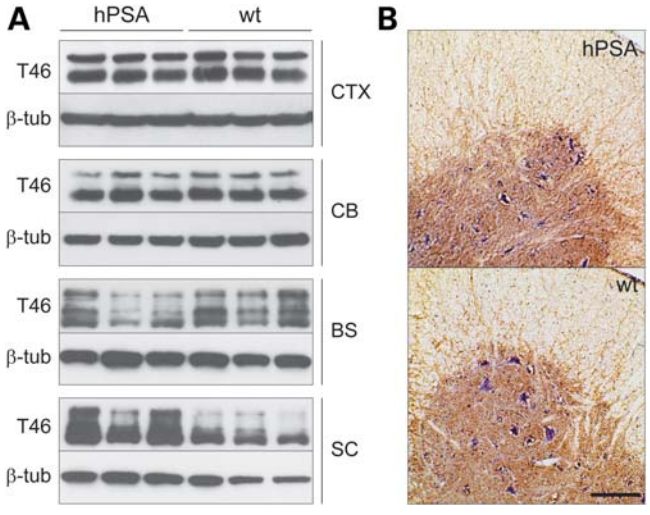

Figure 2. Endogenous total TAU protein levels detected with T46 antibodies are not altered in the hPSA mice. (**A**) Western blot analysis shows no difference in total TAU between 9-month-old hPSA mice and non-transgenic littermate controls in all four CNS regions tested. (**B**) Representative immunohistochemical images of anterior horn spinal cords from 9-month-old hPSA and non-transgenic control mice (wt). CTX, cortex; CB, cerebellum; B, brain stem; SC, spinal cord. The size bar is 100 μm.

hPSA/TAU^{P301L} double-transgenic mice demonstrate delayed paralysis, improved motor neuron density, reduced gliosis and decreased TAU accumulation in the spinal cord

To examine the effects of PSA/NPEPPS overexpression on the development of TAU-induced neurodegeneration *in vivo,* hPSA mice were crossed with TAU^{P301L} transgenic mice (18). As expected, resulting hPSA/TAU^{P301L} double-transgenic animals had elevated hPSA enzyme activity compared with their TAU^{P301L} littermates ($P < 0.05$; Supplementary Material, Fig. S1D).

TAU^{P301L} mice develop motor deficits, weakness and paralysis by as early as 6 months of age (18). Comparison of age of onset (paralysis) using Kaplan–Meier survival curves for hPSA/TAU^{P301L} ($n = 26$) and TAU^{P301L} ($n = 29$) animals demonstrated a distinct trend for a delayed manifestation of the phenotype (log-rank test; $P = 0.0156$; Fig. 3A), with 58.6% and 30.8% paralysis occurrence by the end of the eighth month of age for TAU^{P301L} and hPSA/TAU^{P301L} mice, respectively. However, when separated by sex, both female (Supplementary Material, Fig. S1E) and male (Supplementary Material, Fig. S1F) hPSA/TAU^{P301L} animals showed a less distinctive trend for a later paralysis onset that did not reach statistical significance with the log-rank test (Supplementary Material, Fig. S1E and F). The latter could be due to the limited number of animals in the female ($n = 37$) and male groups ($n = 18$).

Analysis of hPSA/TAU^{P301L} lumbar spinal cords compared with TAU^{P301L} mice revealed a highly significant ($P = 0.00008$) improvement of anterior horn motor neuron density compared with TAU^{P301L} transgenic mice, which normally show up to 50% reduction in motor neuron density (18) (Fig. 3B–D). In addition, extensive gliosis and axonal degeneration observed in the TAU^{P301L} mice (18) were not

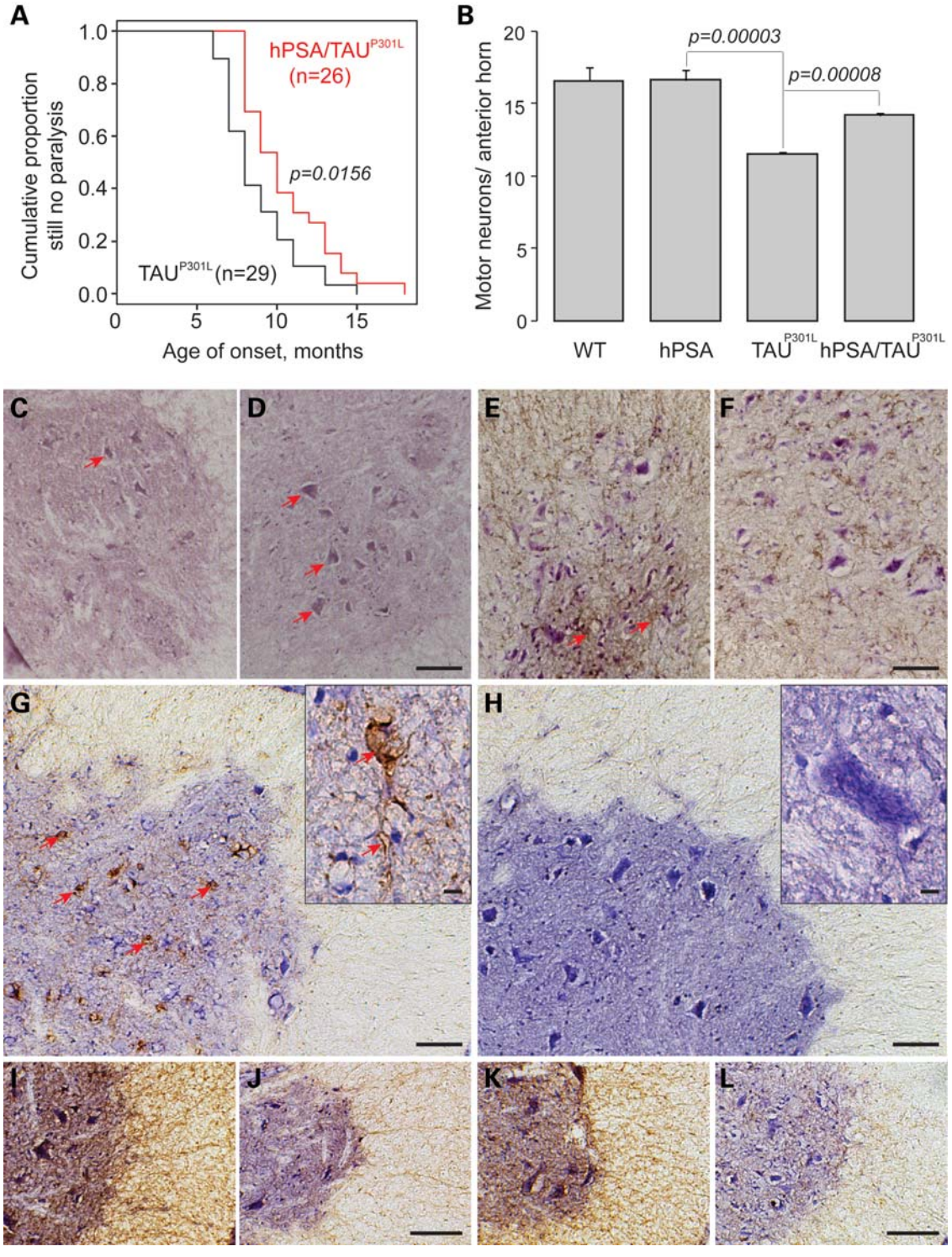

Figure 3. Double-transgenic hPSA/TAU^{P301L} mice show delayed age of onset (paralysis), improved motor neuron counts, no gliosis and reduction of hyperphosphorylated and human-specific TAU protein accumulation in comparison to transgenic TAU^{P301L} mice. (**A**) Kaplan–Meier plots for the age of paralysis onset in TAU^{P301L} ($n = 29$) and hPSA/TAU^{P301L} ($n = 26$) mice demonstrate a trend for the delayed phenotype onset in double-transgenic animals (log-rank test, $P = 0.0156$). (**B**) Double-transgenic hPSA/TAU^{P301L} adult mice (9-months old) demonstrate significantly improved motor neuron density compared with TAU^{P301L} mice ($P = 0.00008$), while motor neuron density between hPSA mice and non-transgenic controls is not significantly different. (**C** and **D**) Representative hematoxylin and eosin-stained images of spinal cord anterior horn sections from 9-month-old TAU^{P301L} (C) and hPSA/TAU^{P301L} double-transgenic mice (D). Note the increased motor neuron density in hPSA/TAU^{P301L} mice. The motor neurons are indicated by red arrows. Compared with TAU^{P301L} mice (**E**), hPSA/TAU^{P301L} double-transgenic mice (**F**) demonstrate reduced gliosis, indicated by GFAP-positive immunostaining. Red arrows indicate areas of extensive gliosis in spinal cord anterior horn of TAU^{P301L} mice. (**G** and **H**) Representative immunohistochemical images using AT8 antibodies show aggregates of hyperphosphorylated TAU in the anterior horn motor neurons of 9-month-old TAU^{P301L} mice (red arrows, G) and absence of TAU-positive staining in littermate hPSA/TAU^{P301L} double-transgenic animals (H). Accumulation of total human TAU observed in the spinal cords of 9-month-old TAU^{P301L} mice (**I** and **K**) is markedly reduced in the hPSA/TAU^{P301L} double-transgenic animals (**J** and **L**) as demonstrated with human TAU-specific antibodies T12 (I and J) and T43D (K, L). The size bar is 100 μm in the lower magnification panels and 10 μm in the higher magnification inserts (G and H).

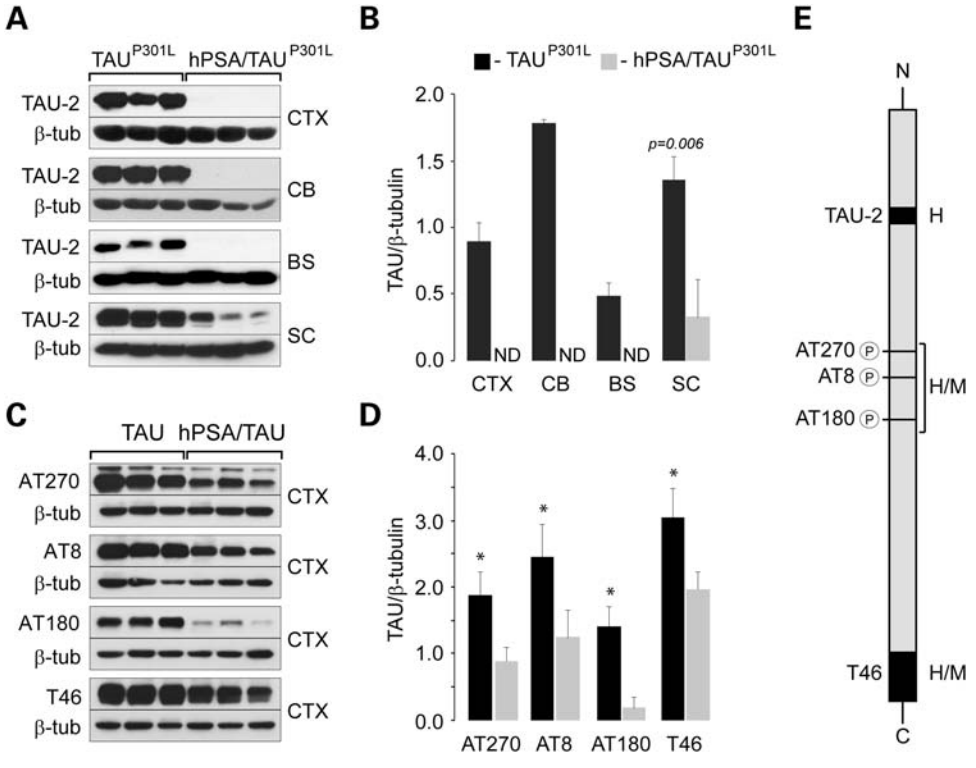

Figure 4. Western blot analysis of 7-month-old hPSA/TAU^{P301L} double-transgenic mice demonstrates significant reduction of soluble human TAU protein compared with TAU^{P301L} littermate controls. Soluble protein fractions from the cortex (CTX), cerebellum (CB), brain stem (BS) and spinal cord (SC) of TAU^{P301L} and hPSA/TAU^{P301L} mice were examined using a panel of antibodies recognizing total human (TAU-2), phosphorylated (AT270, AT8, AT180) and non-phosphorylated (T46) TAU epitopes. (**A** and **B**) Soluble human TAU was nearly absent in most brain regions of double-transgenic mice examined. Trace amounts of human TAU were still detected in the spinal cord tissues. The reduction is most noticeable when human TAU-specific antibodies (TAU-2) are used. (**C** and **D**) Remaining antibodies (AT270, AT8, AT180, T46) recognize both human and mouse TAU; therefore, human-mutated TAU^{P301L} and mouse endogenous TAU isoform are detected as demonstrated with protein extracts isolated from cortex. (**E**) Schematic diagram of antibodies, their specificity (human/mouse) and location of epitopes. ND, not detectable. An asterisk indicates significant difference ($P < 0.01$).

detected in the littermate hPSA/TAU^{P301L} double-transgenic animals (Fig. 3E and F). Furthermore, immunohistochemical analysis of adult (9-month-old) spinal cords demonstrated a substantial reduction of total human (T12 and T43 antibodies; Fig. 3I–L) and hyperphosphorylated (AT8, AT100, AT180, AT270 antibodies) TAU in hPSA/TAU^{P301L} double-transgenic animals as compared with the littermate TAU^{P301L} mice (Figs 3G and H and 4; Supplementary Material, Figs S3–S5).

hPSA/TAU^{P301L} mice demonstrate reduction of soluble human TAU protein

To further understand the behavior of TAU accumulation in hPSA/TAU^{P301L} double-transgenic animals in comparison to the TAU^{P301L} mouse model, we used a battery of TAU-specific antibodies (Supplementary Material, Fig. S2), ample selections of CNS tissues from multiple regions and several different ages corresponding to the early stage of TAU dysfunction (6 months), symptomatic disease stage (9 months) and a stage of advanced neurodegeneration (15 months). First, western blot analysis using human-specific total TAU antibodies (TAU-2) was performed with soluble protein extracts prepared from the cortex, cerebellum, brain stem and spinal cord of 6-month-old hPSA/TAU^{P301L} and TAU^{P301L} littermate control animals. These experiments clearly demonstrated near-complete elimination of human TAU protein from these CNS regions of double transgenic mice (Fig. 4A and B). Analysis of extracts from the cortex of older animals (14 months old) also demonstrated near absence of human TAU protein (Supplementary Material, Fig. S3). Western blot analysis using additional antibodies against hyperphosphorylated (AT270, AT8, AT180) and total (T46) TAU demonstrated a less pronounced but similar trend of lower TAU staining in hPSA/TAU^{P301L} animals (Fig. 4C and D). The latter effect may be explained by the specificity of the antibodies used—only TAU-2 specifically recognizes human TAU, while the others produce signal from both human TAU transgene and endogenous murine TAU protein (Fig. 4E). In addition, TAU-2 antibodies are specific for TAU N-terminus, the region preferentially digested by PSA/NPEPPS (4,5).

Immunohistochemical analysis reveals reduction of hyperphosphorylated TAU aggregates in the brain and spinal cord of hPSA/TAU^{P301L} mice

First, strictly anti-human TAU-specific antibodies were used (T43D and T12; Fig. 3I–L; Supplementary Material, Figs S4 and S5) to look at the tissue- and age-specific distribution of human-specific TAU in hPSA/TAU^{P301L} double-transgenic

mice. As expected, these antibodies produced no staining in hPSA mouse tissues (data not shown). A marked reduction in overall signal from total human TAU was detected in all hPSA/TAU^{P301L} tissues and ages tested as compared with TAU^{P301L} samples (Fig. 3I–L and Supplementary Material, Figs S4 and S5). These data combined with the observation of unaltered levels of endogenous TAU in hPSA transgenic mice (Fig. 2) suggest that the action of hPSA is species-specific and predominantly targets human TAU protein. Hyperphosphorylated TAU-positive staining in different CNS regions of TAU^{P301L} mice (18) recognized by antibodies for phosphorylated TAU epitopes (AT8, AT100, AT180, AT270) was not detected in the hPSA/TAU^{P301L} double-transgenic animals at 6 months (Figs 3G and H and 5A, B, E, F, I and J) or produced markedly reduced or no significant staining at older ages in the double-transgenic animals (Figs 5C, D, G, H, K and L and 6; Supplementary Material, Fig. S6).

PSA/NPEPPS expression directly affects the TAU protein abundance *in vitro*

To investigate the immediate effect of hPSA on TAU protein abundance, a series of hPSA overexpression and RNAi-based inhibition experiments was performed in SH-SY5Y human neuroblastoma cells with follow-up TAU protein analysis at 24, 48 and 72 h post-transfection (Fig. 7). No effect was noticed in the cells incubated for 24 and 48 h post-transfection (data not shown). However, 72 h incubation of cells after transfection with hPSA overexpression vector or hPSA–RNAi constructs resulted in a marked reduction or accumulation of the endogenous TAU protein, respectively, further suggesting that hPSA may be the key peptidase that controls TAU protein abundance in the CNS.

DISCUSSION

We previously demonstrated that PSA/NPEPPS is a novel neuroprotective factor that prevents TAU-induced neurodegeneration through its direct proteolytic function in a fly model of TAU neurotoxicity (4). Importantly, PSA/NPEPPS, being an amino-peptidase, initially cleaves at the N-terminus of TAU (4,5). This is the region of TAU that is most critical for aggregation and for TAU-induced neuropathogenesis (23,24). Here, we reported BAC transgenic mouse lines overexpressing hPSA with no visible pathological phenotype and no significant effect on brain transcriptome, enkephalin turnover, proteasome or autophagy system activity (Fig. 1 and Table 1). Compared with transgenic TAU^{P301L} mice (18), double-transgenic hPSA/TAU^{P301L} animals show a trend for developing the pathological phenotype (paralysis) later in life (Fig. 3A), have improved motor neuron counts (Fig. 3B–D), decreased gliosis (Fig. 3E and F) and markedly reduced accumulation of hyperphosphorylated TAU in all CNS tissues at all ages studied (Figs 3–6 and Supplementary Material, Figs S3–S6).

PSA/NPEPPS is a cytoplasmic and nuclear peptidase with the highest expression in the brain (7,10). It was originally identified as a microtubule-binding peptidase (7,25). Although it was previously suggested that PSA might be an enkephalinase, its intracellular localization precludes PSA from participating in the extracellular enkepahlin processing (11). Insignificant changes in enkephalin degradation rates observed in our hPSA transgenic mice (Fig. 1D) and no changes in enkephalin expression in NPEPPS/PSA-deficient (*PSA*$^{goku/goku}$) mice (12) compared with controls further support this notion. Our hPSA mice of both transgenic lines are born normal, breed normally and do not reveal gross anatomical or behavioral abnormalities, suggesting that current levels of hPSA activation corresponding to ∼2–3-fold may not have any deleterious physiological effects in mammals. Microarray analysis of adult hPSA mice indicates that overexpression of hPSA does not lead to a significant dysregulation of the brain transcriptome (Table 1). Consistent with the role of PSA/NPEPPS in spermatogenesis and gonad development (15,16), one of the two most enriched biological processes in the brain of hPSA mice was sex differentiation (fold enrichment = 6.1, EASE = 0.009). Overall, the observation of a largely unaltered brain transcriptome taken together with the lack of noticeable anatomical or behavioral abnormalities provides additional evidence that at least 2–3-fold hPSA overexpression does not result in any harmful effects, supporting the feasibility of PSA/NPEPPS use as a drug target in mammals.

We demonstrated that constitutive overexpression of hPSA in the TAU^{P301L} mouse model of TAU-induced neurodegeneration results in a delayed disease onset, higher motor neuron density and a significant decrease in mutated TAU protein accumulation. Approximately 90% of TAU^{P301L} mice develop motor deficits, weakness and paralysis by 10 months (18). Characteristic hunched postures are noticed in TAU^{P301L} mice as early as at 6 months (18). Motor neuron density of TAU^{P301L} mice is significantly reduced (∼50%) compared with non-transgenic controls ($P = 0.00003$; Fig. 3B) (18). On the other hand, motor neuron density in hPSA mice is not significantly different from non-transgenic controls ($P = 0.98$; Fig. 3B). Examination of hPSA/TAU^{P301l} mice for neuropathological changes at the tissue level revealed that motor neuron counts are significantly improved ($P = 0.00008$; Fig. 3B–D) compared with TAU^{P301L} mice. Furthermore, although not highly significant (log-rank test, $P = 0.0156$; Fig. 3A), probably because of the limited number of animals examined ($n = 55$) and great individual and sex-specific phenotypic variability among TAU^{P301L} mice (L.C. Kudo, unpublished observation), the time of paralysis occurrence in hPSA/TAU^{P301L} mice shows a clear trend for a delayed age of onset (10.3 months) compared with TAU^{P301L} mice (9.4 months; Fig. 3A). Gliosis (GFAP immunoreactivity), characteristic of TAU^{P301L} mice (18), was not observed in the spinal cord of 6- and 9-month-old hPSA/TAU^{P301L} double-transgenic mice (Fig. 3F). Protein assays of brain soluble fractions demonstrated a significant reduction in human total and hyperphosphorylated protein TAU in the adult (6- and 9--month-old; Fig. 4) and 15-month-old double-transgenic mice (Supplementary Material, Fig. S5). Similar assays using crude protein extracts did not show significant changes in the TAU protein abundance (data not shown), perhaps due to inability of PSA/NPEPPS to digest insoluble aggregated TAU protein. Further immunohistochemical analysis for the presence of hyperphosphorylated TAU and NFTs using a battery of

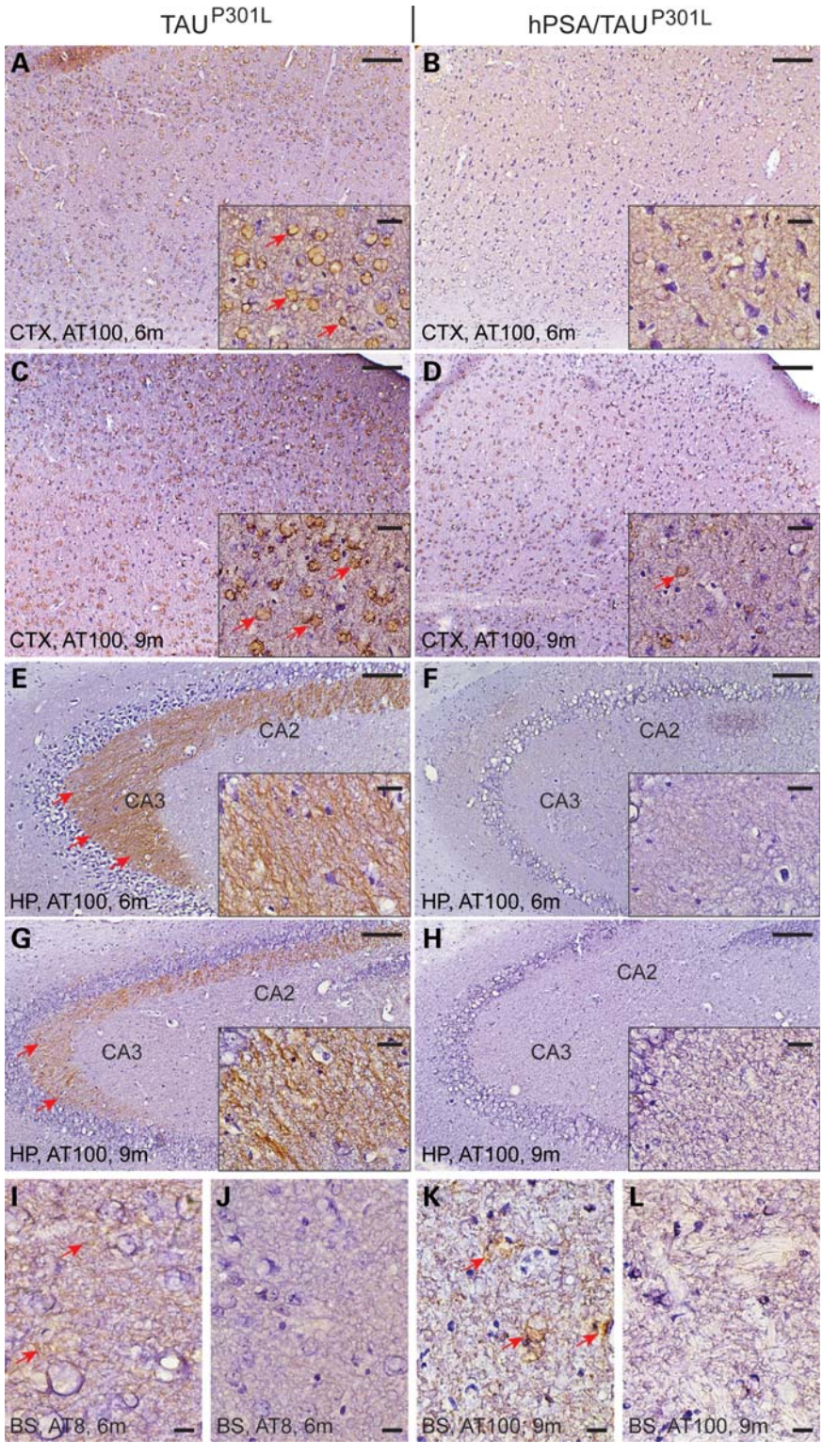

Figure 5. Immunohistochemical analysis demonstrates reduced staining for hyperphosphorylated TAU in the cortex (**A**–**D**), hippocampus (**E**–**H**) and brain stem (**I**–**L**) of 6- and 9-month-old hPSA/TAU^{P301L} (B, D, F, H, J and L) transgenic mice compared with TAU^{P301L} (A, C, E, G, I and K) transgenic mice. (A–D) Representative immunohistochemical images of motor cortex stained for hyperphosphorylated TAU using AT100 antibodies. The representative images demonstrate TAU-positive inclusions in 6- (A) and 9-month-old (C) TAU^{P301L} transgenic mice. hPSA/TAU^{P301L} double-transgenic mice show no accumulation of hyperphosphorylated TAU at the age of 6 months (B) and reduced staining at 9 months (D). (E–H) Representative sections from the hippocampus of 6- (E and F) and 9-month-old (G and H) TAU^{P301L} (E and G) and hPSA/TAU^{P301L} (F and H) mice stained for hyperphosphorylated TAU using AT8 antibodies. Decreased hyperphosphorylated TAU in the CA2 and CA3 areas of hPSA/TAU^{P301L} (F and H) mice is evident. (I–J) Representative brain stem sections from 6- (I and J) and 9-month-old (K and L) TAU^{P301L} (I and K) and hPSA/TAU^{P301L} (J and L) mice immunoreacted with AT8 (I and J) and AT100 (K and L) antibodies. For hPSA/TAU^{P301L} mice, no TAU staining at 6 months (J) and reduced TAU staining at 9 months are shown (L). Arrows indicate the areas of intense hyperphosphorylated TAU staining in TAU^{P301L} transgenic mice. CTX, cortex; HP, hippocampus; BS, brain stem; 6m, 6-month-old animals; 9m, 9-month-old animals. Size bars are 100 μm for images (A)–(H), 10 μm for (I)–(L) and 20 μm for higher magnification inserts.

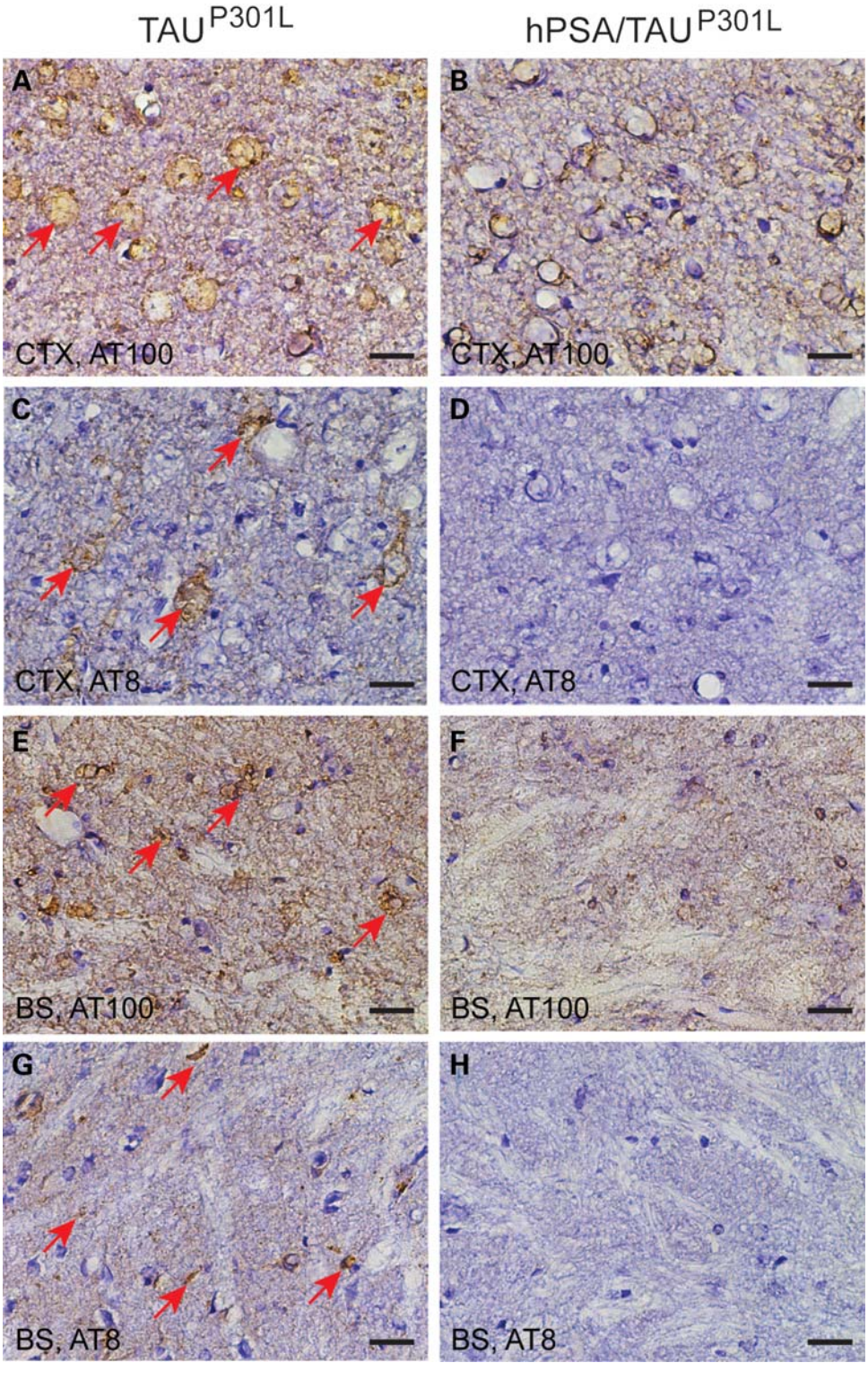

Figure 6. Representative immunohistochemical images demonstrate reduced hyperphosphorylated TAU detected with AT100 (**A**, **B**, **E** and **F**) and AT8 (**C**, **D**, **G** and **H**) antibodies in the motor cortex and brain stem of 15-month-old hPSA/TAU^{P301L} compared with littermate TAU^{P301L} controls. CTX, motor cortex; BS, brain stem. The scale bar is 20 μm.

antibodies which recognize various epitopes showed reduced staining and few TAU-positive deposits in the double-transgenic mice at all ages tested (Figs 3, 5 and 6 and Supplementary Material, Figs S4–S6). Depending on the antibody and brain region, either complete elimination (e.g. AT8 in spinal cord and cortex) or significant reduction (AT100, AT180) of hyperphosphorylated TAU protein and TAU-positive aggregates was detected in all ages of

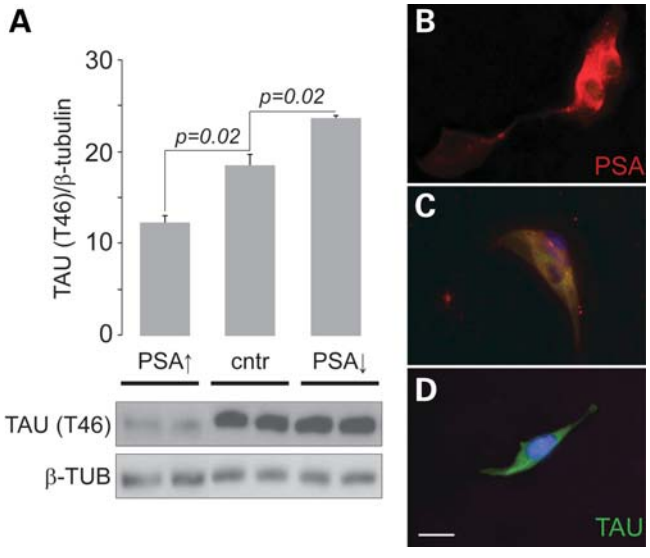

Figure 7. Overexpression of hPSA leads to reduction, while knockdown of hPSA gene expression using siRNA results in a rapid accumulation of TAU protein in SH-SY5Y human neuroblastoma cell lines. (**A**) Western blot analysis shows significant TAU protein reduction in SH-SY5Y cell lines transfected with hPSA overexpression vector (PSA↑) while knockdown of PSA/NPEPPS gene expression using PSA/NPEPPS-specific siRNA (PSA↓) leads to rapid TAU protein accumulation. (**B–D**) Representative immunocytochemical images of SH-SY5Y cells overexpressing PSA/NPEPPS (red) show no staining for TAU protein (green) (B), and cells transfected with empty vector (control) (**C**) and cells transfected with hPSA-specific siRNA (PSA↓) demonstrate accumulation of TAU protein (D). PSA/NPEPPS is red; TAU is green and DAPI nuclear staining is blue. The scale bar is 10 μm.

hPSA/TAU^{P301L} transgenic mice compared with TAU^{P301L} littermate animals (Figs 3–6). These results strongly suggest that hyperphosphorylated TAU is effectively degraded by hPSA/NPEPPS *in vivo*.

Recently, it was demonstrated that proteolysis of TAU protein in SH-SY5Y cells is attenuated following treatment of cells with the hPSA inhibitor puromycin or hPSA-directed siRNA (26). Our *in vitro* experiments in SH-SY5Y cell lines using hPSA overexpression and RNAi-based hPSA knockdown confirmed the hypothesis that TAU protein abundance is directly controlled by hPSA (Fig. 7). While hPSA/NPEPPS overexpression led to the reduction of endogenous TAU protein, knockdown of hPSA/NPEPPS expression resulted in its rapid accumulation (Fig. 7). The latter suggests that dysfunctional hPSA may be an additional contributory factor in TAU-induced neurodegeneration, potentially capable of exacerbating the accumulation of TAU protein.

Our combined data imply that PSA/NPEPPS activation can ameliorate the accumulation of hyperphosphorylated and toxic TAU *in vivo* in mammals. Therefore, increasing PSA/NPEPPS activity may be a feasible therapeutic approach to inhibit and/or block TAU-induced neurodegeneration and thus may provide an effective means to treat tauopathies, including AD. The confirmation here that PSA/NPEPPS can protect from TAU neurotoxicity in mammals *in vivo* and can directly regulate TAU abundance *in vitro* may be analogous to the neuroprotective role of proteolytic processing of other toxic peptides such as amyloid by presenilins, secretases or neprilysin (27,28). Interestingly, PSA/NPEPPS was originally isolated as a candidate β-secretase (29), but its role in amyloid-beta production was not confirmed in follow-up studies (30). However, PSA/NPEPPS co-localization with senile plaques in AD brain (31) and its primary role in the removal of polyglutamine peptides linked to a number of neurodegenerative diseases (13) point to the presence of multiple PSA/NPEPPS targets involving other neurotoxic misfolded proteins and peptides such as amyloid-beta. Indeed, recent work demonstrates that PSA/NPEPPS elevation may efficiently remove various neurotoxic substrates including polyQ-expanded huntingtin exon-1, ataxin-3, mutant α-synuclein and SOD1 *in vitro* (14).

PSA/NPEPPS as a cytoplasmic peptidase may act as a proteasome chaperone at least in the case of polyglutamine repeats (13) and may be involved in the regulation of the autophagic protein clearance (14). However, lack of proteosome and autophagy system activation observed in the hPSA mice together with insignificant changes in autophagic activity under normal physiological conditions reported earlier (14) suggests that both pathways of protein clearance are not regulated by PSA/NPEPPS directly but may employ PSA/NPEPPS at some level to facilitate the removal of unwanted protein species prone to the formation of toxic misfolded aggregates.

Another recent paper reported an unsuccessful attempt to digest TAU protein using *in vitro*-purified PSA/NPEPPS (32). While explanations may be multiple and would include the lack of experimental replicates, the investigators' method of PSA/NPEPPS purification involving sonication and the presence of tagged TAU protein substrate potentially affecting PSA/NPEPPS substrate recognition, it is plausible that the interaction of PSA/NPEPPS with TAU may require intermediate and still unidentified components. However, in our hPSA transgenic mice, the major physiological protein processing and clearance systems of ubiquitin-proteosome and autophagy are not affected (Fig. 1), whereas the accumulation of TAU is almost eliminated by overexpressed hPSA in hPSA/TAU^{P301L} double-transgenic mice (Figs 3–6 and Supplementary Material, Figs S4–S7). These *in vivo* results in mammals combined with our and other's *in vitro* studies (Fig. 5) (4,5,26) strongly suggest that PSA/NPEPPS itself is able to hydrolyze TAU proteins directly and is the key TAU protease; nevertheless, it is possible that besides its direct TAU proteolytic activity, PSA/NPEPPS facilitates TAU clearance in the CNS through the regulation of other unknown protease(s) or pathway(s), which would require additional studies to verify.

Whether PSA/NPEPPS represents an independent global neuroprotective mechanism or acts in concert with other protein clearance pathways, its ability to remove TAU and other toxic proteins/peptides directly in combination with its brain-preferred expression and seemingly low toxicity makes this enzyme an attractive therapeutic target in a wide range of neurodegenerative diseases characterized by abnormal accumulation of TAU and possibly other misfolded and neurotoxic proteins.

MATERIALS AND METHODS

Ethics statement

All animal protocols were in accordance with the NIH Guide for the Care and Use of Laboratory Animals and were

approved by the UCLA animal studies committee. Mice were housed in groups of up to four per cage and kept on a 12 h light/dark cycle at 22°C. Food pellets and water were available *ad libitum*. In this study, 3-, 6-, 9- and 15-month-old animals were used.

TAU^{P301L} transgenic mice

The TAU^{P301L} strain (Taconic), originally obtained from Michael Hutton's group (18), was maintained by breeding hemizygous TAU^{P301L} mutant mice to the non-transgenic B6D2F1 strain. TAU^{P301L} mice express the longest 4R0N isoform of the most commonly found FTDP-17 TAU mutation (P301L) encoding for four-repeat TAU without N-terminal inserts under the control of the mouse prion promoter (33,34). TAU^{P301L} mice demonstrate TAU protein hyperphosphorylation and accumulation of NFTs accompanied by motor neuron degeneration in the spinal cord starting at 6 months, with more moderate pathology in the motor cortex. Motor deficits are detected in transgenic TAU^{P301L} hemizygous mice as early as 6 months, which correlate with significantly reduced motor neuron density in the spinal cord (18).

BAC hPSA transgenic mice

BAC hPSA transgenic mice on FVB/N inbred background were generated following the procedure described in Yang and Gong (20). A 190 kb human BAC (RP11-592D23) containing the full-length 100 kb hPSA coding region, 44 kb 5′ flanking region and 46 kb 3′ flanking sequence was obtained from the BACPAC resource center (Oakland Children's Hospital, Oakland, CA, USA). The BAC was purified from bacterial cultures using standard cesium chloride gradient or Nucleobond BAC Maxi purification kit (Clontech, CA, USA). Purified BAC-DNA was diluted to 3 ng/μl in microinjection buffer (5 mM Tris−HCl, pH 7.4, 10 mM NaCl, 0.1 mM EDTA), microinjected into fertilized mouse (FVB/N) eggs and re-implanted into pseudo-pregnant females at the UCLA Transgenic Core Facility (http://tmc.ctrl.ucla.edu/tg-core/). Three series of injections were performed and the BAC-NPEPPS founders (hPSA mice) were identified using hPSA-specific primers for 5′UTR, 3′UTR, exons 3, 5 and 8 (Supplementary Material, Table S1). Three identified transgenic founders harboring full-length hPSA/NPEPPS were expanded on the FvB background producing hPSA1, hPSA2 and hPSA3 transgenic lines. hPSA1 and hPSA2 lines were crossed with TAU^{P301L} transgenic mice. Breeding, including weaning at 3 weeks and genotyping, was performed according to established protocols**.** Only the first generation of hPSA/TAU^{P301L} double-transgenic mice was used in all experiments. Only littermate animals were used for the comparisons between hPSA/TAU^{P301L}, TAU^{P301L}, hPSA and non-transgenic controls.

PSA/NPEPPS enzymatic activity assay

Two fluorescent substrates, Leu-naphthylamine (βNA) and Leu-AMC, were used for measurements of PSA/NPEPPS enzymatic activities. For the Leu-naphthylamine protocol, the post-microsomal (S_3) extracts of the cerebral cortex, brain stem, cerebellum, kidney, liver and muscle (0.4 mg) in 50 mM Bicine buffer, pH 7.0, in the presence of 0.2 mM DTT were submitted to the FPLC-aminopeptidase analyzer equipped with a Mono Q column (35,36). After the injection, the column was washed for 1 min with Bicine buffer and then eluted with a linear NaCl gradient that increased from 0 to 0.21 M at 12 min, 0.23 M at 26 min, 0.24 M at 36 min, 0.29 M at 56 min and 0.5 M at 61 min. The enzyme elution from the FPLC was mixed with 0.05 mM Leu-βNA and incubated on-line in a delaying coil for 3 min at 37°C. Finally, the elution containing the released fluorescent naphthylamine (ex. 250/em. 389 nm) was measured with a Kratos FS970 spectrofluorometer. The method detected as little as 100 pg of aminopeptidase (37).

For measurements of PSA/NPEPPS activity using Leu-AMC substrate, dissected tissue samples were homogenized manually on ice using a glass homogenizer in 50 mM Bicine buffer (pH 7.0, with 0.2 mM DTT), then centrifuged at 12 000*g* for 30 min at 4°C. The supernatant was collected and protein concentration was measured with Quick Start Bradford Protein Assay Kit according to the manufacture's manual (Bio-Rad, Hercules, CA, USA). To measure PSA/NPEPPS activity, 10 μg of protein of each sample was incubated with fluorescent substrate Leu-AMC (Bachem, Torrance, CA, USA; 100 μM final) at 37°C for 1 h in 96-well plates. The liberated AMC fluorescence was measured on a Synergy 2 Microplate Reader (BioTek, Winooski, VT, USA; ex./em. = 380/460 nm). Bicine buffer without brain extracts was used as the blank control.

MEK degradation assay

The enkephalin degradation rates were measured in whole-brain extracts of adult (6-month-old) hPSA and corresponding non-transgenic littermate control animals. At least three independent animals were used for each brain region and genotype. Two different transgenic lines (hPSA1 and hPSA2) were analyzed. The hydrolysis of MEK was assayed as described previously (38). In brief, the S_3 fraction (25 μl) from 0.3 mg of tissues was incubated with 6.25 nmol of MEK in 75 μl of Bicine buffer for 30 min. The reaction was terminated by adding 25 μl of 5% perchloric acid. After centrifugation, the supernatant was assayed for the disappearance of the substrate. MEK was measured by HPLC using a Waters Radial-Pak C_8 column and monitored by UV absorption at 280 nm. The sample was eluted isocratically at 1 ml/min in ambient temperature with a mixture of acetonitrile and 0.1 M phosphate buffer, pH 3.0 (25:75).

Proteasome and autophagy activity assay

The proteasome activity was measured in the cortex, brain stem and spinal cord of adult (6-month-old) hPSA and corresponding non-transgenic littermate control animals. At least three independent animals were used for each brain region and genotype. The proteasome activity assay was performed as described previously (39). Briefly, 1 μg of crude protein extract was incubated for 30 min at 37°C in the media containing 50 mM Tris (pH 8.0), 1 mM DTT and 40 μM SucLeuLeuValTyr-AMC proteasome fluorogenic substrate.

Released fluorogenic molecule AMC was measured at ex. 370 nm and em. 410 nm. For the measurements of autophagy activity, western blot analysis using LC3 antibodies detecting both cytosolic (LC3-I) and autophagosome (LC3-II) membrane-bound isoforms was used as described previously (40). Conversion of LC3-I to LC3-II corresponding to the activation of autophagy is estimated by measurements of LC3-II/LC3-I relative ratios in the crude protein extracts.

RNA isolation and microarray analysis

For gene expression experiments, the cerebellum and cortex of 6-month-old hPSA1 ($n = 4$) and corresponding non-transgenic littermate males ($n = 4$) were used. Total RNA was extracted using acid phenol extraction (Trizol LS; GIBCO/BRL). The concentration and quality of RNA were determined using the Nanodrop spectrophotometer and confirmed on the Agilent Bioanalyzer. Agilent Whole Mouse Genome Microarray comparisons of the cerebellum and cortex were performed between hPSA transgenic and corresponding non-transgenic (control) littermate animals, producing two independent comparison groups—cerebellum and cortex. Each comparison used four pairs of hPSA transgenic versus corresponding control littermate animals, producing four biological replicates. Raw microarray data were acquired using the Agilent DNA Microarray scanner and processed with the accompanying Agilent Feature Extraction 10.5 Image Analysis software using default settings (see the MIAME report). Normalized signal intensities were used to identify gene expression changes in the cerebellum and cortex of adult 6-month-old hPSA mice, generating two partially overlapping sets of data. For the identification of differential expression, the genes were required to pass two conservative criteria: a ratio beyond the 95% confidence interval observed in homotypic comparisons (4,41–43), which corresponded to an ~1.5-fold expression change, and a paired *t*-test ($P < 0.01$) computed using 100 permutations of the data for each gene. Correction for multiple comparisons was performed using the adjusted Bonferroni test. The analysis was performed in the TM4: Microarray Software Suite (http://www.tm4.org/; (44). For further details on data analyses, see the MIAME report.

GO and pathway analysis

To assess the relevance of the identified gene expression changes, searches for GO-based, overrepresented functional groups were performed using the Database for Annotation, Visualization, and Integrated Discovery (DAVID) (http://david.abcc.ncifcrf.gov/) (45). To avoid the errors due to duplicated genes, the Fisher exact statistics was calculated based on corresponding DAVID gene IDs. The significance of enrichment or the EASE score was a modified Fisher exact *P*-value with Benjamini correction for multiple comparisons. Only categories with an EASE score below 0.01 were considered significant.

Age of paralysis onset and motor neuron density

To estimate whether the age of phenotypic onset (paralysis) is significantly different due to overexpression of PSA/NPEPPS, transgenic TAU^{P301L} ($n = 29$) and $hPSA/TAU^{P301L}$ double-transgenic mice ($n = 26$) were monitored for over 17 months. The age of paralysis was recorded for each animal and the data were plotted as the Kaplan–Meier survival curve estimate (46) (Fig. 3A) with monthly intervals. To estimate the difference in the age of phenotype onset between two genotypes, a standard log-rank test in the R statistical package was used (47). The analysis was performed in the groups combining both sexes (Fig. 3A) and separately in males and females (Supplementary Material, Fig. S1E and F).

Motor neuron counts were performed on matching lumbar spinal cord anterior horn regions using 12 μm sections of TAU^{P301L}, hPSA1, hPSA2, $hPSA1/TAU^{P301L}$, $hPSA2/TAU^{P301L}$ and non-transgenic mice stained with hematoxylin and eosin. Counts were performed on every fifth section. On average, 18 sections from each animal were counted. At least four 9-month-old female animals were used for each genotype. The results were reflected as the mean of neuronal density (number of neurons per section). The statistical significance was estimated by Student's *t*-tests.

Protein extraction and western blot analysis

The CNS was dissected, separating the spinal cord, cortex, brain stem and cerebellum. For preparation of crude protein extracts, frozen tissue samples were homogenized by sonication in hypotonic buffer (10 mM Tris–HCl, 10 mM KCl, 0.1 mM EDTA, 0.1% Triton X-100, pH 8.0) with protease inhibitor cocktail (Sigma), the protein extracts were centrifuged for 20 min at 10 000*g* at 4°C and supernatants were decanted.

The fractionation of proteins from mouse CNS tissues was performed according to Holzer *et al*. (48) with minor modifications. Briefly, CNS tissue samples were homogenized in ice-cold buffer (20 mM HEPES, pH 7.4, 150 mM NaCl, 25 mM L-glycerol phosphate, 15 mM sodium pyrophosphate, 1 mM EDTA, 1 mM EGTA, 5 mM L-mercaptoethanol, 1 mM PMSF) with a protease inhibitor cocktail (Sigma) and centrifuged for 60 min at 100 000*g* at 4°C. Supernatants were collected and referred to as the soluble cytosolic fraction. The remaining pellets were resuspended in hypotonic buffer (10 mM Tris–HCl, 10 mM KCl, 0.1 mM EDTA, 0.1% Triton X-100, pH 8.0) with protease inhibitor cocktail (Sigma). Protein extracts were centrifuged for 20 min at 10 000*g* at 4°C and supernatants corresponding to 'insoluble fraction' were collected. Protein concentrations in the extracts were determined using Coomassie Protein Assay Reagent (Pierce).

Western blot procedure was performed according to standard protocols. For the identification of PSA/NPEPPS, goat polyclonal anti-PSA (1:200, kindly provided by Dr Hui) and goat polyclonal anti-PSA (1:1000, Millipore) antibodies were used. The panel of anti-TAU antibodies included TAU-2, a mouse monoclonal anti-human TAU (1:200, Sigma), mouse anti-TAU antibody T46 (1:1000, Zymed Laboratories), mouse monoclonal anti-PHF-TAU antibodies AT8 (1:200, MN1020, Pierce), AT180 (1:200, MN1040, Pierce), AT270 (1:1000, MN1050, Pierce) and goat polyclonal anti-TAU V-20 (1:200, Santa Cruz) (Supplementary Material, Fig. S2). For the detection of autophagy activity, rabbit anti-LC3 antibodies were used (1:2000, Novus Biologicals). D66 monoclonal antibodies (1:1000, Sigma) were used to

detect β-tubulin. Secondary antibodies included donkey anti-goat IgG (H + L), goat anti-mouse IgG (H + L) (1:20 000) and goat anti-rabbit IgG (H + L) (1:10 000) all from Jackson ImmunoResearch Laboratories, Inc. Antibodies were detected using the ECL kit (GE). The blots were scanned and quantified using ImageJ. For each comparison, at least three separate experiments were performed and significance was estimated by Student's *t*-tests.

Immunohistochemistry

Perfused mouse brain or spinal cords (PBS followed by 4% paraformaldehyde) were cut into 12 μm sections, placed onto glass slides and air dried for 20 min. Slides were kept at −80° until use. Immunohistochemistry was performed according to standard protocols using Vector Laboratory kits: ABC Elite; DAB; M.O.M. Kit basic. TAU-specific antibodies included TAU-2 (1:50), anti-human TAU antibody T12 (1:500, Covance) and T43 (1:1000, Covance), AT8 (1:50), AT180 (1:25), AT100 (1:200, MN1060, Pierce), AT270 (1:100), V-20 (1:200) and T46 (1:500) (Supplementary Material, Fig. S2). In addition, mouse anti-neuronal nuclei (NeuN) monoclonal antibody (1:100; Chemicon) and GFAP (1:500; Dako) were used. Secondary biotinylated antibodies included polyclonal horse anti-mouse (1:250, Vector Laboratory), goat anti-rabbit (1:200, Vector Laboratory) and rabbit anti-goat (1:100, Vector Laboratory).

In vitro experimentation

SH-SY5Y human neuroblastoma cell lines (American Type Culture Collection, VA, USA) characterized by stable expression of hPSA/NPEPPS and TAU proteins were used for both hPSA/NPEPPS overexpression and inhibition experiments. The cultures were maintained in DMEM/F12 (1:1) (GIBCO) with 10% HI FBS (GIBCO) and 1% penicillin/streptomycin (GIBCO) according to standard methodology.

For overexpression experiments, the pCMV6-XL vector (OPEN Biosystems) carrying full-length hPSA cDNA (NM_006310) was purified using NucleoBond Endotoxin-free plasmid DNA purification kit (MACHEREY-NAGEL). Transfections were performed using Lipofectamine 2000 (Invitrogen, CA, USA) according to manufacturer's recommendations. For each 10^5 cells, 1 μg of the PSA/NPEPPS-pCMV6-XL vector was used.

For gene inhibition/knockdown experiments, a mixture of three predesigned siRNA oligonucleotides was used (no. 129900, Stealth RNAi, Invitrogen). Efficient hPSA/NPEPPS silencing (at least 70% inhibition, 24 h post-transfection) was confirmed with both real-time PCR and western blot analysis. Block-It Fluorescent Transfection kit (Invitrogen), which provides non-toxic Lipofectamine2000 reagent and Block-IT Fluorescent double-stranded RNA oligomer as an indicator of transfection efficiency, was used for siRNA transfection. For each 10^5 cells, 20 pmol of siRNA mixture was used. After transfection with both plasmid and siRNA, cells were harvested after 24, 48 and 72 h of incubation.

All experiments were performed at least three times with several replicates ($n > 3$) in each experiment. Western blot assay of total TAU in the protein extracts from SH-SY5Y cells transfected with hPSA overexpression vectors, control vectors or hPSA-siRNA was performed with T46 antibodies (1:1000; Invitrogen) according to standard protocols. Immunocytochemistry was performed according to the protocol of Glynn and McAllister (49) using goat anti-PSA polyclonal (1:1000; Millipore) and mouse anti-TAU T46 (1:200; Invitrogen) primary antibodies. The secondary antibodies were rabbit anti-goat IgG (H + L) Alexa Fluor 568 (1:2000; Invitrogen) and rabbit anti-mouse IgG (H + L) Alexa Fluor 488 (1:2000; Invitrogen).

SUPPLEMENTARY MATERIAL

Supplementary Material is available at *HMG* online.

ACKNOWLEDGEMENTS

The authors would like to thank Dr Elizabeth Neufeld and Dr Patricia Dickson for critical reading of the manuscript.

Conflict of Interest statement. None declared.

FUNDING

The work was supported by the UCLA Alzheimer Research Centre (S.L.K.), the CurePSP Society (S.L.K.), RGK Foundation (S.L.K.), UCLA Older Americans Independence Center (S.L.K. and L.P.), Liu Young Investigator Award (S.L.K.), Alzheimer Association (S.L.K. and L.C.K.) and NARSAD (S.L.K.).

REFERENCES

1. Ballatore, C., Lee, V.M. and Trojanowski, J.Q. (2007) Tau-mediated neurodegeneration in Alzheimer's disease and related disorders. *Nat. Rev. Neurosci.*, **8**, 663–672.
2. Brunden, K.R., Ballatore, C., Crowe, A., Smith, A.B. 3rd, Lee, V.M. and Trojanowski, J.Q. (2010) Tau-directed drug discovery for Alzheimer's disease and related tauopathies: a focus on tau assembly inhibitors. *Exp. Neurol.*, **223**, 304–310.
3. Brunden, K.R., Trojanowski, J.Q. and Lee, V.M. (2009) Advances in tau-focused drug discovery for Alzheimer's disease and related tauopathies. *Nat. Rev. Drug Discov.*, **8**, 783–793.
4. Karsten, S.L., Sang, T.K., Gehman, L.T., Chatterjee, S., Liu, J., Lawless, G.M., Sengupta, S., Berry, R.W., Pomakian, J., Oh, H.S. *et al.* (2006) A genomic screen for modifiers of tauopathy identifies puromycin-sensitive aminopeptidase as an inhibitor of tau-induced neurodegeneration. *Neuron*, **51**, 549–560.
5. Sengupta, S., Horowitz, P.M., Karsten, S.L., Jackson, G.R., Geschwind, D.H., Fu, Y., Berry, R.W. and Binder, L.I. (2006) Degradation of tau protein by puromycin-sensitive aminopeptidase *in vitro*. *Biochemistry*, **45**, 15111–15119.
6. Hersh, L.B. and McKelvy, J.F. (1981) An aminopeptidase from bovine brain which catalyzes the hydrolysis of enkephalin. *J. Neurochem.*, **36**, 171–178.
7. Constam, D.B., Tobler, A.R., Rensing-Ehl, A., Kemler, I., Hersh, L.B. and Fontana, A. (1995) Puromycin-sensitive aminopeptidase. Sequence analysis, expression, and functional characterization. *J. Biol. Chem.*, **270**, 26931–26939.
8. Thompson, M.W., Tobler, A., Fontana, A. and Hersh, L.B. (1999) Cloning and analysis of the gene for the human puromycin-sensitive aminopeptidase. *Biochem. Biophys. Res. Commun.*, **258**, 234–240.
9. Dyer, S.H., Slaughter, C.A., Orth, K., Moomaw, C.R. and Hersh, L.B. (1990) Comparison of the soluble and membrane-bound forms of the

puromycin-sensitive enkephalin-degrading aminopeptidases from rat. *J. Neurochem.*, **54**, 547–554.
10. McLellan, S., Dyer, S.H., Rodriguez, G. and Hersh, L.B. (1988) Studies on the tissue distribution of the puromycin-sensitive enkephalin-degrading aminopeptidases. *J. Neurochem.*, **51**, 1552–1559.
11. Hui, K.S. (2007) Brain-specific aminopeptidase: from enkephalinase to protector against neurodegeneration. *Neurochem. Res.*, **32**, 2062–2071.
12. Osada, T., Ikegami, S., Takiguchi-Hayashi, K., Yamazaki, Y., Katoh-Fukui, Y., Higashinakagawa, T., Sakaki, Y. and Takeuchi, T. (1999) Increased anxiety and impaired pain response in puromycin-sensitive aminopeptidase gene-deficient mice obtained by a mouse gene-trap method. *J. Neurosci.*, **19**, 6068–6078.
13. Bhutani, N., Venkatraman, P. and Goldberg, A.L. (2007) Puromycin-sensitive aminopeptidase is the major peptidase responsible for digesting polyglutamine sequences released by proteasomes during protein degradation. *EMBO J.*, **26**, 1385–1396.
14. Menzies, F.M., Hourez, R., Imarisio, S., Raspe, M., Sadiq, O., Chandraratna, D., O'Kane, C., Rock, K.L., Reits, E., Goldberg, A.L. *et al.* (2010) Puromycin-sensitive aminopeptidase protects against aggregation-prone proteins via autophagy. *Hum. Mol. Genet.*, **19**, 4573–4586.
15. Lyczak, R., Zweier, L., Group, T., Murrow, M.A., Snyder, C., Kulovitz, L., Beatty, A., Smith, K. and Bowerman, B. (2006) The puromycin-sensitive aminopeptidase PAM-1 is required for meiotic exit and anteroposterior polarity in the one-cell *Caenorhabditis elegans* embryo. *Development*, **133**, 4281–4292.
16. Fortin, S.M., Marshall, S.L., Jaeger, E.C., Greene, P.E., Brady, L.K., Isaac, R.E., Schrandt, J.C., Brooks, D.R. and Lyczak, R. (2010) The PAM-1 aminopeptidase regulates centrosome positioning to ensure anterior-posterior axis specification in one-cell *C. elegans* embryos. *Dev. Biol.*, **344**, 992–1000.
17. Towne, C.F., York, I.A., Neijssen, J., Karow, M.L., Murphy, A.J., Valenzuela, D.M., Yancopoulos, G.D., Neefjes, J.J. and Rock, K.L. (2008) Puromycin-sensitive aminopeptidase limits MHC class I presentation in dendritic cells but does not affect CD8 T cell responses during viral infections. *J. Immunol.*, **180**, 1704–1712.
18. Lewis, J., McGowan, E., Rockwood, J., Melrose, H., Nacharaju, P., Van Slegtenhorst, M., Gwinn-Hardy, K., Paul Murphy, M., Baker, M., Yu, X. *et al.* (2000) Neurofibrillary tangles, amyotrophy and progressive motor disturbance in mice expressing mutant (P301L) tau protein. *Nat. Genet.*, **25**, 402–405.
19. Gong, S. and Yang, X.W. (2005) Modification of bacterial artificial chromosomes (BACs) and preparation of intact BAC DNA for generation of transgenic mice. *Curr. Protoc. Neurosci.*, Chapter 5, Unit 5 21.
20. Yang, X.W. and Gong, S. (2005) An overview on the generation of BAC transgenic mice for neuroscience research. *Curr. Protoc. Neurosci.*, Chapter 5, Unit 5 20.
21. Osada, T., Watanabe, G., Kondo, S., Toyoda, M., Sakaki, Y. and Takeuchi, T. (2001) Male reproductive defects caused by puromycin-sensitive aminopeptidase deficiency in mice. *Mol. Endocrinol.*, **15**, 960–971.
22. Osada, T., Watanabe, G., Sakaki, Y. and Takeuchi, T. (2001) Puromycin-sensitive aminopeptidase is essential for the maternal recognition of pregnancy in mice. *Mol. Endocrinol.*, **15**, 882–893.
23. Amadoro, G., Serafino, A.L., Barbato, C., Ciotti, M.T., Sacco, A., Calissano, P. and Canu, N. (2004) Role of N-terminal tau domain integrity on the survival of cerebellar granule neurons. *Cell Death Diff.*, **11**, 217–230.
24. Gamblin, T.C., Chen, F., Zambrano, A., Abraha, A., Lagalwar, S., Guillozet, A.L., Lu, M., Fu, Y., Garcia-Sierra, F., LaPointe, N. *et al.* (2003) Caspase cleavage of tau: linking amyloid and neurofibrillary tangles in Alzheimer's disease. *Proc. Natl Acad. Sci. USA*, **100**, 10032–10037.
25. Hui, K.S., Hui, M., Lajtha, A. and Saito, M. (1990) Cellular localization of puromycin-sensitive aminopeptidase isozymes. *Neurochem. Res.*, **15**, 1147–1151.
26. Yanagi, K., Tanaka, T., Kato, K., Sadik, G., Morihara, T., Kudo, T. and Takeda, M. (2009) Involvement of puromycin-sensitive aminopeptidase in proteolysis of tau protein in cultured cells, and attenuated proteolysis of frontotemporal dementia and parkinsonism linked to chromosome 17 (FTDP-17) mutant tau. *Psychogeriatrics*, **9**, 157–166.
27. Hardy, J. and Selkoe, D.J. (2002) The amyloid hypothesis of Alzheimer's disease: progress and problems on the road to therapeutics. *Science*, **297**, 353–356.
28. Sisodia, S.S. and St George-Hyslop, P.H. (2002) gamma-Secretase, Notch, Abeta and Alzheimer's disease: where do the presenilins fit in? *Nat. Rev. Neurosci.*, **3**, 281–290.
29. Schonlein, C., Loffler, J. and Huber, G. (1994) Purification and characterization of a novel metalloprotease from human brain with the ability to cleave substrates derived from the N-terminus of beta-amyloid protein. *Biochem. Biophys. Res. Commun.*, **201**, 45–53.
30. Huber, G., Thompson, A., Gruninger, F., Mechler, H., Hochstrasser, R., Hauri, H.P. and Malherbe, P. (1999) cDNA cloning and molecular characterization of human brain metalloprotease MP100: a beta-secretase candidate? *J. Neurochem.*, **72**, 1215–1223.
31. Minnasch, P., Yamamoto, Y., Ohkubo, I. and Nishi, K. (2003) Demonstration of puromycin-sensitive alanyl aminopeptidase in Alzheimer disease brain. *Leg. Med. (Tokyo)*, **5** (Suppl. 1), S285–S287.
32. Chow, K.M., Guan, H. and Hersh, L.B. (2010) Aminopeptidases do not directly degrade tau protein. *Mol. Neurodegener.*, **5**, 48.
33. Borchelt, D.R., Davis, J., Fischer, M., Lee, M.K., Slunt, H.H., Ratovitsky, T., Regard, J., Copeland, N.G., Jenkins, N.A., Sisodia, S.S. *et al.* (1996) A vector for expressing foreign genes in the brains and hearts of transgenic mice. *Genet. Anal.*, **13**, 159–163.
34. Trojanowski, J.Q. and Lee, V.M. (1999) Transgenic models of tauopathies and synucleinopathies. *Brain Pathol.*, **9**, 733–739.
35. Hui, K.S., Saito, M. and Hui, M. (1998) A novel neuron-specific aminopeptidase in rat brain synaptosomes. Its identification, purification, and characterization. *J. Biol. Chem.*, **273**, 31053–31060.
36. Hui, M. and Hui, K.S. (2008) A new type of neuron-specific aminopeptidase NAP-2 in rat brain synaptosomes. *Neurochem. Int.*, **53**, 317–324.
37. Hui, K.S. and Hui, M. (1996) An automatic continuous-flow aminopeptidase detector and its applications. *Anal. Biochem.*, **242**, 271–273.
38. Hui, K.S. (1988) A novel dipeptidyl aminopeptidase in rat brain membranes. Its isolation, purification, and characterization. *J. Biol. Chem.*, **263**, 6613–6618.
39. Bousquet-Dubouch, M.P., Nguen, S., Bouyssie, D., Burlet-Schiltz, O., French, S.W., Monsarrat, B. and Bardag-Gorce, F. (2009) Chronic ethanol feeding affects proteasome-interacting proteins. *Proteomics*, **9**, 3609–3622.
40. Tanida, I. and Waguri, S. (2010) Measurement of autophagy in cells and tissues. *Methods Mol. Biol.*, **648**, 193–214.
41. Kudo, L.C., Parfenova, L., Vi, N., Lau, K., Pomakian, J., Valdmanis, P., Rouleau, G.A., Vinters, H.V., Wiedau-Pazos, M. and Karsten, S.L. (2010) Integrative gene-tissue microarray-based approach for identification of human disease biomarkers: application to amyotrophic lateral sclerosis. *Hum. Mol. Genet.*, **19**, 3233–3253.
42. Lobo, M.K., Karsten, S.L., Gray, M., Geschwind, D.H. and Yang, X.W. (2006) FACS-array profiling of striatal projection neuron subtypes in juvenile and adult mouse brains. *Nat. Neurosci.*, **9**, 443–452.
43. Ohmi, K., Kudo, L.C., Ryazantsev, S., Zhao, H.Z., Karsten, S.L. and Neufeld, E.F. (2009) Sanfilippo syndrome type B, a lysosomal storage disease, is also a tauopathy. *Proc. Natl Acad. Sci. USA*, **106**, 8332–8337.
44. Saeed, A.I., Sharov, V., White, J., Li, J., Liang, W., Bhagabati, N., Braisted, J., Klapa, M., Currier, T., Thiagarajan, M. *et al.* (2003) TM4: a free, open-source system for microarray data management and analysis. *Biotechniques*, **34**, 374–378.
45. Huang da, W., Sherman, B.T. and Lempicki, R.A. (2009) Systematic and integrative analysis of large gene lists using DAVID bioinformatics resources. *Nat. Protoc.*, **4**, 44–57.
46. Kaplan, E.L. and Meier, P. (1958) Nonparametric estimation from incomplete observations. *J. Am. Statist. Assoc.*, **53**, 457–481.
47. Harrington, D. (2005) Linear rank tests in survival analysis. In *Encyclopedia of Biostatistics*. Wiley Interscience. DOI: 10.1002/0470011815.b2a11047.
48. Holzer, M., Rödel, L., Seeger, G., Gärtner, U., Narz, F., Janke, C., Heumann, R. and Arendt, T. (2001) Activation of mitogen-activated protein kinase cascade and phosphorylation of cytoskeletal proteins after neurone-specific activation of p21ras. II. Cytoskeletal proteins and dendritic morphology. *Neuroscience*, **105**, 1041–1054.
49. Glynn, M.W. and McAllister, A.K. (2006) Immunocytochemistry and quantification of protein colocalization in cultured neurons. *Nat. Protoc.*, **1**, 1287–1296.